



Modeling Vitexin and Isovitexin Flavones as Corrosion Inhibitors for Aluminium Metal


Abdullahi Muhammad Ayuba

Department of Pure and Industrial Chemistry, Bayero University, Kano, Nigeria, ayubaabdullahi@buk.edu.ng

Umaru Umar

Department of Pure and Industrial Chemistry, Bayero University, Kano, Nigeria

Follow this and additional works at: <https://kijoms.uokerbala.edu.iq/home>

 Part of the [Environmental Chemistry Commons](#), [Environmental Monitoring Commons](#), [Materials Chemistry Commons](#), [Oil, Gas, and Energy Commons](#), and the [Physical Chemistry Commons](#)

Recommended Citation

Ayuba, Abdullahi Muhammad and Umar, Umaru (2021) "Modeling Vitexin and Isovitexin Flavones as Corrosion Inhibitors for Aluminium Metal," *Karbala International Journal of Modern Science*: Vol. 7 : Iss. 3 , Article 4.

Available at: <https://doi.org/10.33640/2405-609X.3119>

This Research Paper is brought to you for free and open access by Karbala International Journal of Modern Science. It has been accepted for inclusion in Karbala International Journal of Modern Science by an authorized editor of Karbala International Journal of Modern Science. For more information, please contact abdulateef1962@gmail.com.

Modeling Vitexin and Isovitexin Flavones as Corrosion Inhibitors for Aluminium Metal

Abstract

Theoretically, the aluminium corrosion inhibitive performance of vitexin (VTX) and isovitexin (SVT) were evaluated with a view of establishing the mechanism of the inhibition process. Calculations which include the consideration of several global descriptors were studied to describe and correlate the reactivity of the molecules with the computed descriptors. First and second-order condensed Fukui functions were employed to analyze local reactivity parameters, while simulations involving the adsorbed molecules on Al (1 1 0) surface were conducted through quench dynamic simulations and the mechanism of physical adsorption was established with SVT relatively been a better inhibitor on Al surface than VTX.

Keywords

Fukui indices, global descriptors, molecular dynamics, quantum parameters

Creative Commons License



This work is licensed under a [Creative Commons Attribution-Noncommercial-No Derivative Works 4.0 License](https://creativecommons.org/licenses/by-nc-nd/4.0/).

Cover Page Footnote

The authors did not receive any funding sources for this research

1. Introduction

Some of the industrial problems resulting from deterioration of metals based installment is due to corrosion, especially when exposed to aggressive medium such as moisture, solutions of bases, acids, salts etc [1]. Industrial processes including cleaning, pickling, oil acidification, chemical and electrochemical etching which involve the use of acid solutions on metals cannot be avoided [2,3]. For this reason, many researchers have devoted ample time and resources in studying the corrosion and corrosion inhibition of one of the most useful metals (aluminium). Aluminium and its alloys are known to find applications in various industrial purposes such as machinery construction, electronics, transport equipment etc due to their low cost, high mechanical properties, good malleability, low density, corrosion resistance, conductivity among others [4–6]. The outer surface of aluminium is known to be characterized by a thin passive oxide film (amphoteric in nature) that provides some immunity against the corrosive environments. This amphoteric layer could be attacked by acid, alkaline or salt solutions and therefore subjecting the metal to corrosion under unfavorable environments. Consequently, there is need to protect and preserve this metal [7,8]. One of the most effective and cost efficient methods of controlling corrosion is the use of inhibitors [9]. Large number of known organic and inorganic compounds have been reportedly used as corrosion inhibitors on aluminium metal, some of which are deleterious to the environment [10]. Most organic compounds carefully selected for the purpose of inhibition are large in size, abundant, inexpensive, environmentally friendly, which are expected to adsorb on the metal surface in order to prevent its direct contact with the aggressive molecules [11]. Factors including aromaticity, electron density, molecular size, functional groups, electronic structure of the molecules and π -orbital character of donating electrons of the compounds are known to enhance their adsorption abilities onto the metal surface [12,13].

The inhibitor adsorption abilities of these organic compounds coupled with their molecular and electronic properties have been directly related to their inhibition efficiencies [14]. The study of relationships between inhibitor structure and inhibition performance is an important theoretical technique which can assist researchers in predicting inhibition efficiencies and designing of promising corrosion inhibitors [15].

Microscopic level explanation of the mechanism of corrosion inhibition through quantum mechanics have been an effective method used in studying the correlation between inhibition efficiency and molecular/electronic structure [16,17]. Recently, the interactions of the adsorbed molecule and that of the metal surface have been successfully modeled using molecular dynamic simulations [18]. These studies revealed that molecular dynamic simulation can provide better insights into the design of inhibitor system with superior properties, and the adsorption/binding energy obtained from the simulation can be used to distinguish the differences in inhibition efficiency of different inhibitor molecules [15].

It is understood from literature that sometimes the influence of the two key factors (structural and electronic) in determining the inhibition efficiency of molecules cannot be easily differentiated, making it very difficult to establish the actual parameter that is responsible for enhancing the inhibition efficiency of the molecules [19,20]. For this reason, this study decided to choose molecules with similar chemical structures (Fig. 1), with the intention of annulling the effect of structural contribution to the possible inhibition efficiency of the selected molecules. With this, parameters related to electronic nature of the molecules were selected and investigated.

The present work is aimed at studying the inhibition action of vitexin (5,7-dihydroxy-2-(4-hydroxyphenyl)-8-((2S,3R,4R,5S,6R)-3,4,5-trihydroxy-6-(hydroxymethyl)-tetrahydro-2H-pyran-2-yl)-4H-chromen-4-one) and isovitexin (5,7-dihydroxy-2-(4-hydroxyphenyl)-6-((2S,3R,4R,5S,6S)-3,4,5,6-tetrahydroxy-tetrahydro-2H-pyran-2-yl)-4H-chromen-4-one) on aluminium metal. In addition, to correlate their inhibition efficiency with some calculated quantum chemical parameters and to carry out molecular dynamic simulations using computational methods.

2. Theory

All geometric optimizations, simulations and theoretical calculations were performed using BIOVIA Inc Material Studio software 8.0. After optimizations, quantum chemical parameters were calculated using the B3LYP functional with DND basis set in DMol³ package of the Density functional theory (DFT) [21,22]. Global reactivity descriptors analyzed include energy of the highest occupied molecular orbital (E_{HOMO}), lowest unoccupied molecular orbital

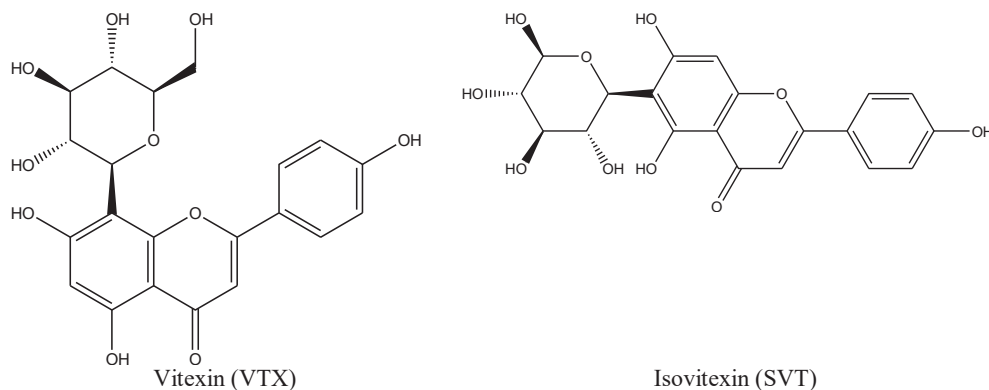


Fig. 1. Molecular structure of the studied inhibitor compounds.

(E_{LUMO}), separation energy (ΔE), dipole moment (μ), and those parameters that give information about the molecular reactivity, such as electronegativity (χ), ionization potential (I), electron affinity (A), hardness (η), softness (σ), and fraction of electrons transferred from the inhibitor molecule to metal surface (ΔN).

2.1. Global reactivity descriptors

The number of electrons (N) of a system that has a total energy (E) at a constant external potential $v(r)$ can be used to calculate the chemical potential (μ) of such a system. Eq. (1) shows the relationship between μ and electronegativity (χ) in terms of first derivative of E with N at constant $v(r)$ [23]:

$$\chi = -\mu = -\left(\frac{\partial E}{\partial N}\right)_{v(r)} \quad (1)$$

The second derivative of Eq. (1) at constant $v(r)$ can be used to define hardness (η) as presented in Eq. (2) [24,25]:

$$\eta = \left(\frac{\partial E^2}{\partial N^2}\right)_{v(r)} = \left(\frac{\partial \mu}{\partial N}\right)_{v(r)} \quad (2)$$

E_{HOMO} and E_{LUMO} can be related to ionization potential (I) and electron affinity (A) using Koopman's theorem, as in Eq. (3) and Eq. (4) [26,27]:

$$I = -E_{HOMO} \quad (3)$$

$$A = -E_{LUMO} \quad (4)$$

With finite difference approximation, I and A can be used to calculate χ and η as in Eq. (5) and Eq. (6) [28]:

$$\chi = \frac{(I+A)}{2} = -\frac{E_{LUMO} + E_{HOMO}}{2} \quad (5)$$

$$\eta = \left(\frac{I-A}{2}\right) = -\frac{E_{LUMO} - E_{HOMO}}{2} \quad (6)$$

The inverse of chemical hardness ($\sigma = 1/\eta$) is defined as the global softness and can be used to measure the extent of polarizability [29,30].

Parameters such as fraction of electrons transferred from inhibitor molecule to the metal surface (ΔN), global electrophilicity index (ω), nucleophilicity (ϵ) and the energy of back donation (ΔE_{b-d}) were derived from global hardness and electronegativity as in Eqs. 7–10 [31]:

$$\Delta N = \frac{\chi_{Al} - \chi_{inh}}{2(\eta_{Al} + \eta_{inh})} \quad (7)$$

$$\omega = \frac{\mu^2}{2\eta} = \frac{\chi^2}{2\eta} \quad (8)$$

$$\epsilon = \frac{1}{\omega} \quad (9)$$

$$\Delta E_{b-d} = -\frac{\eta}{4} = \frac{1}{8}(E_H - E_L) \quad (10)$$

Where χ_{Al} and χ_{inh} represent absolute electronegativities of aluminium and inhibitor molecule, while η_{Al} and η_{inh} are the hardness of aluminium and inhibitor molecule respectively. The theoretical value of electronegativity of bulk aluminium is 5.6eV while the hardness value is 0eV [32], this is by assuming that for a metallic bulk ($I = A$) because they are softer than neutral metallic atoms [33].

2.2. Fukui functions

In order to evaluate the local reactivity regions of the studied molecules, Fukui indices were explored to

locate the regions where electrophilic and nucleophilic attacks are likely to occur. Fukui indices have been defined as the first derivative of the density of electrons of a system $\rho(\mathbf{r})$ with respect to the total number of electrons (N) at a fixed external potential $v(\mathbf{r})$ as given in Eq. (11) [34]:

$$f(\mathbf{r}) = \left[\frac{\partial \rho(\mathbf{r})}{\partial N} \right] v(\mathbf{r}) = \left[\frac{\partial \mu}{\partial v(\mathbf{r})} \right] v(\mathbf{r}) \quad (11)$$

Roy et al. [35], on the other hand defined the electrophilic, nucleophilic and radical Fukui functions for site k in a molecule by using left and right derivatives with respect to the number of electrons (N) as in Eq. 12–14 for nucleophilic, electrophilic and radical attack respectively:

$$f_{k(r)}^+ = \rho_K(N + 1) - \rho_K(N) \quad (12)$$

$$f_{k(r)}^- = \rho_K(N) - \rho_K(N - 1) \quad (13)$$

$$f_{k(r)}^o = \frac{\rho_K(N + 1) - \rho_K(N - 1)}{2} \quad (14)$$

Where ρ_K is the gross charge of the atom k in the molecule, N is the number of electrons in the molecule, $N+1$ corresponds to an anion with an electron added to the LUMO of the neutral molecule, $N-1$ corresponds to a cation after removal of an electron from the HOMO of the neutral molecule [34].

Second order Fukui function (f^2) known as the dual descriptor $\Delta f(k)$, is another local descriptor introduced by Morell et al. [36]. It has been defined as the difference between nucleophilic and electrophilic Fukui functions as in Eq. (15):

$$f^2(\mathbf{r}) = f_k^+ - f_k^- \quad (15)$$

If $f^2(\mathbf{r}) > 0$, then site k prefers nucleophilic attack, whereas if $f^2(\mathbf{r}) < 0$, then site k prefers an electrophilic attack [37]. This indicates that $f^2(\mathbf{r})$ serves as an index of selectivity towards nucleophilic or electrophilic attacks [36].

2.3. Molecular dynamic simulation

The interaction between inhibitor molecules and the aluminium surface was studied by executing quench molecular dynamic simulation using the Forcite module in BIOVIA Material Studio 8.0. The interaction between the optimized structures of the molecules and Al(110), were used for the simulation [38]. Al(110) is the most densely packed and most stable among the different forms of aluminium [39]. The interaction

between the Al(110) and inhibitor molecules was carried out in simulation box ($9 \times 6 \text{ \AA}$) with periodic boundary conditions [33], a vacuum slab of 20 \AA height was mounted on the Al(110). Simulations were carried out using the condensed-phase optimized molecular potentials for atomistic simulation studies (COMPASS) force field and the smart algorithm at 350 K in an NVT conical ensemble with time step of 1fs and simulation time of 5 ps [38]. The system was quench every 250 steps. During the simulation process, all the bulk atoms in the Al(110) surface were constrained so that only the surface atoms are allowed to interact with the inhibitor molecules freely [39]. The aluminium slab built for the simulation process is significantly larger than the molecules in order to avoid edge effects [39]. The adsorption energy was calculated according to Eq. (16) [32]:

$$E_{adsorption} = E_{total} - (E_{inhibitor} + E_{surface}) \quad (16)$$

Where E_{total} is the total energy of inhibitor and metal surface, $E_{surface}$ is the energy of Al surface without inhibitor molecule, $E_{inhibitor}$ is the energy of free inhibitor molecule. Binding energy is the negative value of the adsorption energy:

$$E_{binding} = - E_{adsorption} \quad (17)$$

3. Results and discussion

3.1. Global reactivity descriptors

Analyzing global reactivity descriptors such as frontier molecular orbital, orbital energies and electronic distributions are considered the most significant results of density functional theory study that can be used to predict the reactivity of any inhibitor molecule with respect to a suitable metal [40]. These parameters are discussed under the following headings:

3.1.1. Frontier molecular orbitals

The snap shots of the geometry optimized molecules, HOMO, LUMO and total electron density distributions of the two studied inhibitor molecules are presented in Figs. 2 and 3. The optimized electronic structures correspond to the global energy minima of the studied molecules with no imaginary frequencies [31]. From the figures it can be observed that the geometry optimized structures for the two molecules are almost planar. This planarity gives the molecules ideal orientation for strong interaction and orientation with the aluminium metal surface [40]. The HOMO

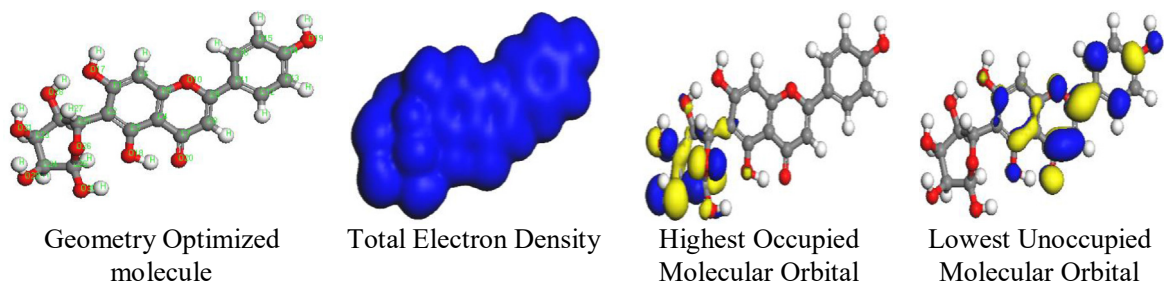


Fig. 2. Structural and global reactivity properties of SVT.

indicates the regions of the molecule with tendency to donate electrons to the empty orbitals of the aluminium metal, whereas the LUMO points out the regions of the molecule with ability to accept electrons from d-orbitals of the aluminium metal by back bonding [29]. The shapes of the HOMO and LUMO are very significant in predicting the reactivity of the inhibitor molecules [41]. From Figs. 2 and 3, it can be observed that both HOMO and LUMO of the two molecules are distributed on oxygen atoms and aromatic rings of the molecules, this signifies their tendency to take part in the process of donation and acceptance of electrons [37]. The HOMO orbitals are relatively more distributed on oxygen atoms when compared to aromatic rings of the studied molecules, indicating a better ability of oxygen atoms in donating electrons when compared to aromatic rings, this is due to the availability of lone pair of electrons. By observing the structures in Figs. 2 and 3, the following conclusions can be drawn:

- i. Oxygen atoms in the two molecules participate better in donation than acceptance of electrons.
- ii. Both the two molecules can be effective corrosion inhibitors owing to their ability to donate as well as accept electrons during their interaction with the aluminium metal.

However, by comparing the bond angles of bent planes in the two molecules (Fig. 4), it can be observed

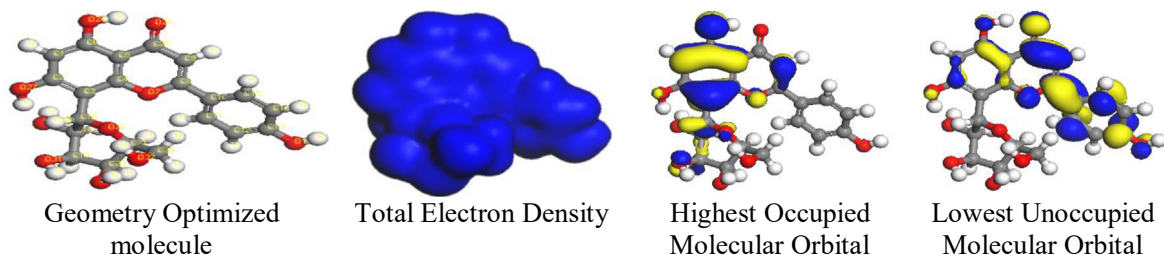


Fig. 3. Structural and global reactivity properties of VTX.

that VTX has larger bond angles than SVT. The bond angles formed by $C_1-C_2-C_{21}$, $C_6-C_5-O_{10}$, $C_9-C_{11}-C_{12}$ and $C_9-C_{11}-C_{16}$ in SVT are 125.375, 119.873, 119.229 and 118.182° respectively, whereas, in VTX, the bond angles formed by $C_4-C_3-C_{16}$, $O_7-C_8-C_{10}$, $C_8-C_{10}-C_{15}$ and $C_3-C_2-O_{27}$ are 125.447, 121.060, 119.472 and 120.726° respectively. The relatively lower bond angle values of SVT when compared to VTX is an indication of its better planarity which enhances flat lying orientation with expected stronger adsorption energy [32].

3.1.2. Frontier molecular orbital energies

The frontier molecular orbital energies obtained from quantum chemical calculations are presented in Table 1. It can be observed that, SVT has higher value of E_{HOMO} and therefore is expected to have better inhibition efficiency when compared to VTX. The energy gap ($\Delta E = E_L - E_H$) is a significant descriptor that determines the reactivity of molecules towards metal surface [42]. Reactivity of molecules increases as ΔE value decreases, because the energy required to remove an electron from last occupied molecular orbital is less [43], thus, molecules with low ΔE values are expected to have better inhibition performance. It is also known that molecules with low ΔE values are more polarizable with high chemical reactivity [39]. SVT has less ΔE value, hence is likely to be more effective as corrosion inhibitor than VTX (Table 1).

Chemical hardness (η) is the resistance against electron cloud polarization [44], therefore as the

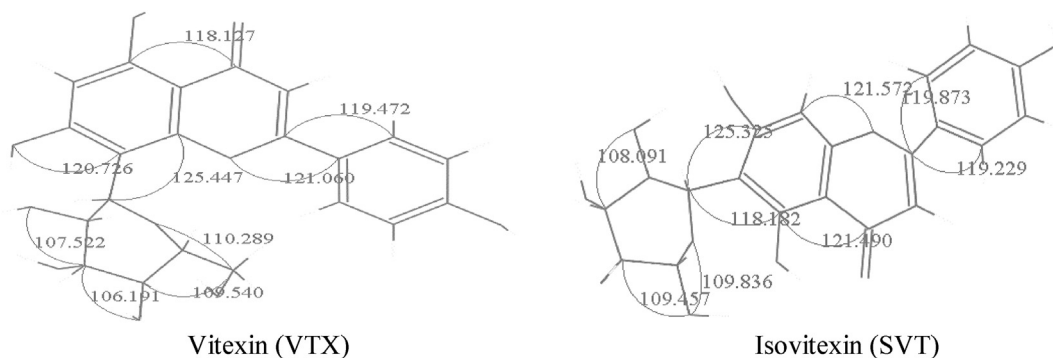


Fig. 4. Bond angles in the studied molecules.

hardness (η) value of molecule increases, its inhibition efficiency decreases since hard molecules resist electron donation. In contrary to the above, soft molecules are good corrosion inhibitors, the greater the softness, the higher the inhibition efficiency [45]. From the results presented in Table 1, the order of inhibition efficiency of the studied molecules in terms of hardness and softness follows SVT > VTX. Dipole moment (μ) of a molecule is related to the polarity of polar covalent bonds [46]. It is defined as the product of charge and the distance between the two concerned atoms [47]. According to literature, there are many disagreements in correlation of dipole moment with inhibition efficiency of inhibitor molecules [48]. As can be observed from Table 1, VTX has higher value of dipole moment when compared to SVT. The fraction of electron transferred from the inhibitor molecule to metal surface (ΔN) was calculated according to Pearson method

as described in Eq. (7) [49] and the results are presented in Table 1. It has been reported by Verma et al. [50] that, if $0 < \Delta N > 3.6$, the inhibitor molecule has strong tendency to donate electrons to the empty orbitals of the metal. According to the values of ΔN in Table 1, it is evident that both inhibitor molecules can donate electrons to the vacant orbitals of aluminium to form coordinate bonds, with SVT having stronger bond with aluminium due to its higher value of ΔN . Ionization potential (I) and electron affinity (A) of the inhibitor molecules were calculated according to Eq. (3) and Eq. (4) respectively by the application of Koopman's theorem [51]. These two values were used in calculating electronegativity and global hardness of the respective molecules.

Energy of back donation (ΔE_{b-d}) is another important parameter that describes the interaction of inhibitor molecules with metal surface. The back donation process was proposed by Gomez et al. [52]. Bedair [53] reported that if the value of global hardness is positive and ΔE_{b-d} is negative, then the process of back donation is favored. Values of global hardness for both molecules presented in Table 1 are positive while that of back donation are negative, suggesting that the interaction of the inhibitor molecules with aluminium surface involves the transfer of charge from inhibitor molecules to aluminium metal and vice versa as pointed out by Umaru and Ayuba [48]. On the basis of results from the energy of back donation, the inhibition efficiency of the molecules obeys the trend SVT > VTX which is in agreement with parameters earlier discussed.

Electrophilicity index (ω) indicates the ability of the molecules to accept electrons, whereas nucleophilicity (ϵ) which is the inverse of electrophilicity ($1/\omega$) represents the propensity of the molecules to donate or share electrons [48]. It is known that molecules with

Table 1
Calculated quantum chemical parameters of the studied inhibitor molecules

Properties	Inhibitor molecules	
	VTX	SVT
HOMO (at orbital number)	113	109
LUMO (at orbital number)	114	110
E_{HOMO} (eV)	-5.116	-4.919
E_{LUMO} (eV)	-2.582	-2.942
ΔE (eV)	2.534	1.977
Dipole moment (Debye)	3.045	2.967
Ionization potential (I) (eV)	5.116	4.919
Electron affinity (A) (eV)	2.582	2.942
Global hardness (η) (eV)	1.267	0.989
Global softness (σ) (eV ⁻¹)	0.789	1.012
Absolute electronegativity (χ) (eV)	3.849	3.931
Fraction of electrons transferred (ΔN)	0.691	0.845
Electrophilicity index (ω) (eV)	5.846	7.814
Nucleophilicity (ϵ) (eV ⁻¹)	0.171	0.128
Energy of back donation (ΔE_{b-d}) (eV)	-0.317	-0.247

large values of electrophilicity index are poor corrosion inhibitors while molecules with high values of nucleophilicity are good corrosion inhibitors [31]. Table 1 reported large values of electrophilicity index of the molecules which is due to the high reliance of B3LYP functional on electronegativity, consequently these two parameters cannot be used to infer any sequence about the inhibition efficiency of the studied molecules as suggested by Guo et al. [31].

3.2. Fukui functions

Local reactivity of the studied molecules has been investigated by the use of Fukui indices to indicate the active centers of the molecules with respect to nucleophilic and electrophilic attack. High values of f^+ mark the points of nucleophilic attack, while high values of f^- indicate the points of electrophilic attacks in the molecule [25]. The condensed Fukui functions of the molecules are presented in Table 2. From this table, it can be observed that, in VTX: C₈, C₁₃, O₁₇ and O₂₆ which possess high values of absolute f^+ charge (0.076, 0.046, 0.043 and 0.075 respectively) are the active centers for nucleophilic attack. C₁, C₃, O₂₄ and O₂₇ on the other hand are the sites where electrophiles are expected to attack the molecule, because they bear the highest absolute f^- charge values (0.056, 0.081, 0.114 and 0.041 respectively). For SVT, the nucleophilic centers are located on C₇(0.055), C₉(0.078), C₁₄(0.045) and O₂₀(0.075) while the electrophilic sites are located on O₂₆(0.106), O₂₉(0.210) and O₃₁(0.052). Based on the analyzed Fukui functions, it can be stated that VTX and SVT have several points of nucleophilic and electrophilic attacks in their structures, therefore both can be good inhibitor molecules with superiority attributed to SVT.

Second order Fukui function (f^2) is another significant local reactivity parameter. The computed values of second order Fukui functions are depicted in Table 2 and graphically presented in Figs. 5 and 6. Through these figures and Table 2, it can be observed that in VTX, 61.29% of the elements in the figure show positive values of second order Fukui functions ($f^2 > 0$) while 38.71% of the elements show negative values ($f^2 < 0$). Such values for SVT have 70.97% of the elements in the figure revealing positive values of second order Fukui functions, while 22.58% exhibited negative values. In view of this, it can be concluded that SVT is more nucleophilic than VTX, and therefore more effective in inhibiting the corrosion of aluminium metal surface [31]. Herein, the order for inhibition efficiency remains as earlier discussed.

Table 2

Condensed Fukui and second-order Fukui functions of the studied molecules.

VTX				SVT			
Atom	f^+	f^-	f^2	Atom	f^+	f^-	f^2
C(1)	0.026	0.056	-0.030	C(1)	0.021	0.010	0.011
C(2)	0.018	0.013	0.005	C(2)	0.023	-0.020	0.043
C(3)	0.025	0.081	-0.056	C(3)	0.024	0.006	0.018
C(4)	-0.002	0.033	-0.035	C(4)	0.007	0.003	0.004
C(5)	0.010	0.033	-0.023	C(5)	-0.001	0.015	-0.016
C(6)	0.015	0.022	-0.007	C(6)	0.022	0.014	0.008
O(7)	0.027	0.024	0.003	C(7)	0.055	0.005	0.050
C(8)	0.076	0.004	0.072	C(8)	0.023	0.007	0.016
C(9)	0.033	0.030	0.003	C(9)	0.078	0.002	0.070
C(10)	0.004	-0.005	0.009	O(10)	0.030	0.006	0.024
C(11)	0.028	0.003	0.025	C(11)	-0.003	-0.002	-0.001
C(12)	0.014	0.007	0.007	C(12)	0.027	0.002	0.025
C(13)	0.046	0.013	0.033	C(13)	0.015	0.005	0.010
C(14)	0.012	0.009	0.003	C(14)	0.045	0.007	0.028
C(15)	0.030	0.004	0.026	C(15)	0.011	0.006	0.005
C(16)	-0.007	-0.005	-0.002	C(16)	0.037	0.004	0.033
O(17)	0.043	0.023	0.020	O(17)	0.023	-0.011	0.034
C(18)	0.001	-0.008	0.009	O(18)	0.032	-0.028	0.060
C(19)	0.003	-0.011	0.014	O(19)	0.045	0.014	0.031
C(20)	0.001	-0.012	0.013	O(20)	0.075	0.010	0.065
C(21)	-0.004	-0.013	0.009	C(21)	-0.005	-0.029	0.024
O(22)	-0.001	0.009	-0.010	C(22)	-0.004	-0.001	-0.003
O(23)	0.011	0.014	-0.003	C(23)	-0.006	-0.020	0.014
O(24)	0.037	0.114	0.023	C(24)	0.000	-0.038	0.038
C(25)	0.047	0.012	0.035	C(25)	-0.008	-0.022	0.014
O(26)	0.075	0.037	0.038	O(26)	0.008	0.106	-0.098
O(27)	0.035	0.041	-0.006	O(28)	0.013	0.020	-0.007
O(29)	0.007	0.012	-0.005	O(29)	0.013	0.210	-0.197
C(30)	0.008	-0.002	0.010	O(30)	0.018	0.039	-0.021
O(31)	0.008	0.025	-0.017	O(31)	0.009	0.052	-0.043

Note: f^+ corresponds to nucleophilic site; f^- corresponds to electrophilic site; f^2 represents second order Fukui function.

3.3. Molecular dynamic simulation

To study the nature of interactions between inhibitor molecules and aluminium surface, Forcite quench molecular dynamic simulation was employed. Geometry optimization of the system was first performed, followed by molecular dynamic simulation process after temperature and energy values reached equilibrium, sampling of quenched trajectories was conducted and the average of five lowest energies were recorded [48]. The adsorption and binding energies of the molecules on Al(110) surface were calculated according Eq. (16) and Eq. (17) respectively, the values obtained are as presented in Table 3. Large negative values of adsorption energy imply a better adsorption ability of inhibitors and thus typically higher inhibition performance [25,29]. Table 3 reported large negative values of adsorption energies for both inhibitors which

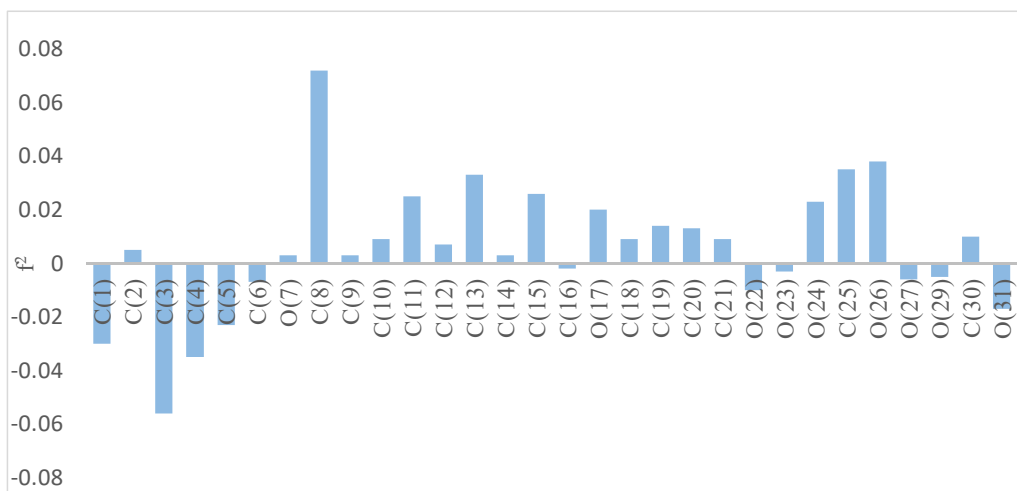


Fig. 5. Second-order Fukui functions of SVT.

is an indication of strong and spontaneous interaction between the inhibitor molecules and Al(110) surface [48]. Comparing the adsorption energies of the two molecules, it can be observed that, SVT is negatively larger than VTX, this suggests its ability to have a stronger and more stable interaction with Al(110) surface [39]. It has been reported in literature that adsorption energies negatively greater than -100 kcal/mol are associated with chemical adsorption, while values lower than that signify physical adsorption [25,29]. Based on the values of adsorption energies of the molecules in Table 3, it can be concluded that both molecules are physically adsorbed onto the Al(110)

surface, therefore vander Waals forces of interaction are proposed to be the mechanism of the association of the molecules with the Al(110) surface.

The lowest energy optimized equilibrium adsorption configurations of both molecules on Al(110) surface are presented in Fig. 7. SVT molecule can be observed to be relatively better adsorbed (flat orientation) on Al(110) surface with the aromatic ring and the oxygen atoms of the molecule having a close contact with the surface. This is in agreement with the results discussed earlier in this work from frontier molecular orbitals, global and local reactivity values of the molecules with the order: SVT > VTX.

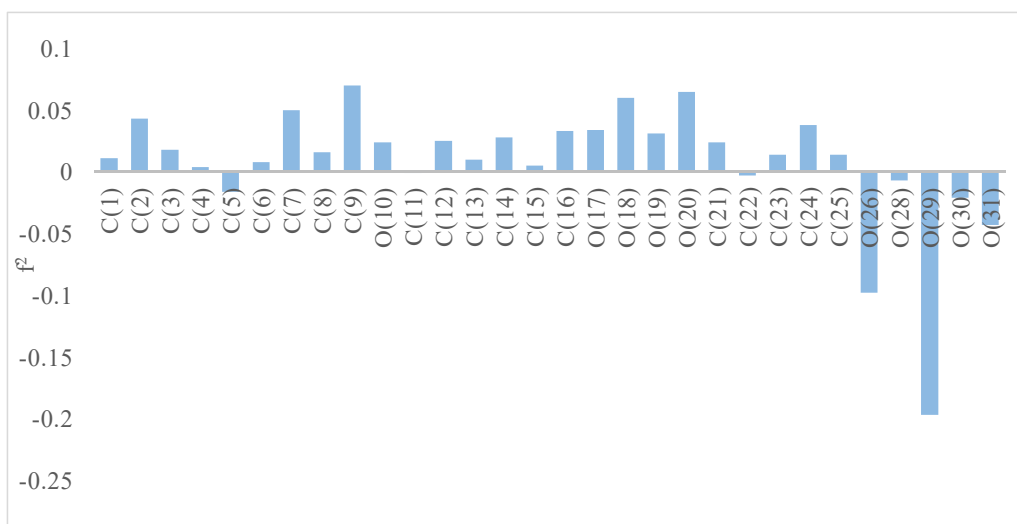


Fig. 6. Second-order Fukui functions of VTX.

Table 3
Computed adsorption parameters for the interaction of the studied molecules with the Al (110) surface.

Properties	Molecules	
	SVT	VTX
Total potential energy (kcal/mol)	-115.968 ± 5.222	-102.631 ± 4.774
Energy of molecule (kcal/mol)	-55.464 ± 0.0155	54.849 ± 0.0108
Energy of Al (110) surface (kcal/mol)	0.0000 ± 0.0000	0.0000 ± 0.0000
Adsorption energy (kcal/mol)	-60.504 ± 0.0151	-47.782 ± 0.0105
Binding energy (kcal/mol)	60.504 ± 0.0151	47.782 ± 0.0105

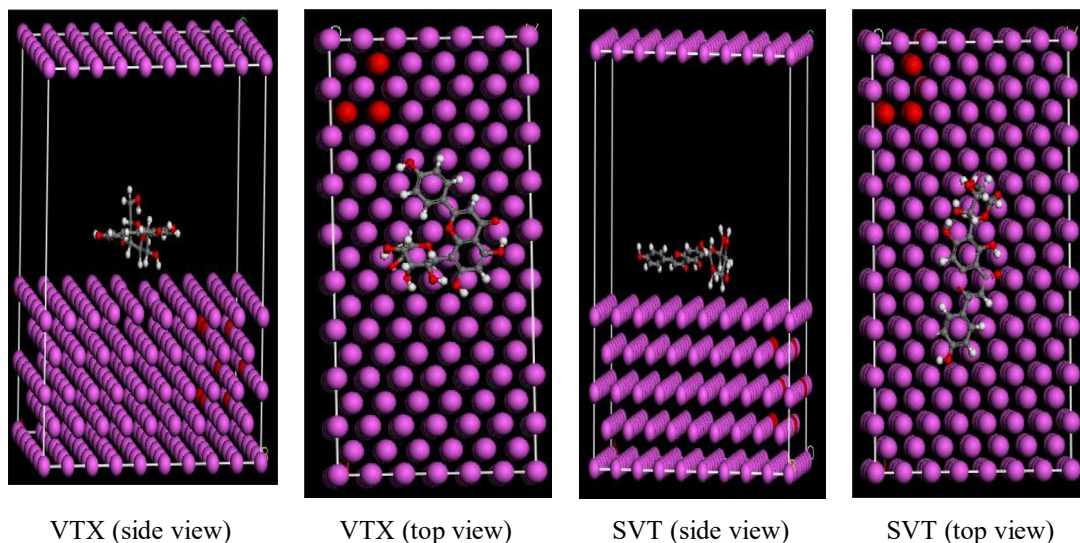


Fig. 7. Equilibrium adsorption configurations of studied molecules on Al(110).

4. Conclusion

In this work, quantum chemical calculations and molecular dynamic simulations were employed to predict the inhibitive properties of vitexin (VTX) and isovitexin (SVT) against the corrosion of aluminium metal. The results obtained from this study using global and local reactivity indices revealed that both molecules are potentially good corrosion inhibitors and both can adsorb onto the surface of the metal through a mechanism of physical adsorption. Even though both SVT and VTX are isomers, results have revealed that SVT is relatively a better inhibitor on Al surface than VTX, possibly due to its electronic distribution and planar structure which render it favorable surface coverage on the metal surface resulting into better orientation and adsorption interaction strength.

Conflicts of interest

Authors have declared that, there is no conflict of interest in this work.

Acknowledgement

We are very grateful to all staff in the Department of Pure and Industrial Chemistry Bayero University Kano, Nigeria for their assistance in running this work.

References

- [1] A. Dehghani, A.H. Mostafatabar, G. Bahlakeh, B. Ramezanzadeh, M. Ramezanzadeh, Detailed-level computer modelling explorations complemented with comprehensive experimental studies of Quercetin as a highly effective inhibitor for acid-induced steel corrosion, *J. Mol. Liq.* 309 (2020) 113035, <https://doi.org/10.1016/j.molliq.2020113035>.
- [2] K.F. Khaled, A.A. Muhammad, Electrochemical and molecular dynamic simulation studies on the corrosion inhibition of aluminium in molar hydrochloric acid using some imidazole derivatives, *J. Appl. Electrochem.* 39 (2009) 2553–2568, <https://doi.org/10.1007/s10800-009-9951-x>.
- [3] X. Luo, C. Ci, J. Li, K. Lin, S. Du, H. Zhang, X. Li, Y.F. Cheng, J. Zang, Y. Liu, 4-aminoazobenzene modified natural glucomannan as a green eco-friendly inhibitor for the mild steel in 0.5 M HCl solution, *Corros. Sci.* 151 (2019) 132–142, <https://doi.org/10.1016/j.corsci.2019.02.027>.

- [4] A.Y. Musa, A.A.H. Kadhum, A.B. Mohamad, M.S. Takriff, A. R. Daud, S.K. Kamarudin, On the inhibition of mild steel corrosion by 4-amino-5-phenyl-4H-1,2,4-triazole-3-thiol, *Corros. Sci.* 52 (2010) 526–533, <https://doi.org/10.1016/j.corsci.2009.10.009>.
- [5] R. Rosliza, W.B.W. Nik, S. Izman, Y. Prawoto, Anti-corrosive properties of natural honey on Al–Mg–Si alloy in seawater, *Curr. Appl. Phys.* 10 (2010) 923–929, <https://doi.org/10.1016/j.cap.2009.11.074>.
- [6] J.A. Hill, T. Markley, M. Forsyth, P.C. Howlett, B.R.W. Hinton, Corrosion inhibition of 7000 series aluminium alloys with cerium diphenyl phosphate, *J. Alloys Compd.* 509 (2011) 1683–1690, <https://doi.org/10.1016/j.jallcom.2010.09.151>.
- [7] J. John, S.A. Joseph, Quantum chemical and electrochemical studies on the corrosion inhibition of aluminium in 1 N HNO₃ using 1,2,4-triazine, *Mater. Corros.* 64 (2013) 625–632, <https://doi.org/10.1002/maco.201206782>.
- [8] M.M. Al-Qahtani, K.F. Khaled, The inhibitive effect of some tetrazole derivatives towards Al Corrosion in acid solution: chemical, electrochemical and theoretical studies, *Mater. Chem. Phys.* 113 (2009) 150–158, <https://doi.org/10.1016/j.matchemphys.2008.07.060>.
- [9] P.B. Raja, M. Ismai, S. Ghoreishiamiri, J. Mirza, M.C. Ismail, S. Kakooei, et al., Reviews on corrosion inhibitors: a short view, *Chem. Eng. Commun.* 203 (2016) 1145–1156, <https://doi.org/10.1080/00986445.2016.1172485>.
- [10] S.A. Umoren, I.B. Obot, A. Madhankumar, Z.M. Gasem, Performance evaluation of pectin as ecofriendly corrosion inhibitor for X60 pipeline steel in acid medium: experimental and theoretical approaches, *Carbohydr. Polym.* 124 (2015) 280–291, <https://doi.org/10.1016/j.carbpol.2015.02.036>.
- [11] H. Ju, Z.P. Kai, Y. Li, Aminic nitrogen-bearing polydentate Schiff base compounds as corrosion inhibitors for iron in acidic media: a quantum chemical calculation, *Corros. Sci.* 50 (2008) 865–871, <https://doi.org/10.1016/j.corsci.2007.10.009>.
- [12] M.E. Belghiti, A. Dafali, Y. Karzazi, M. Bakasse, H. Elaloui-Elabdallaoui, L.O. Olasunkanmi, E.E. Ebenso, Computational simulation and statistical analysis on the relationship between corrosion inhibition efficiency and molecular structure of some hydrazine derivatives in phosphoric acid on mild steel surface, *Appl. Surf. Sci.* 491 (2019) 707–722, <https://doi.org/10.1016/j.apsusc.2019.04.0125>.
- [13] M. Jayalakshmi, V.S. Muralidharan, Correlation between structure and inhibition of organic-compounds for acid corrosion of transition-metals, *Indian J. Chem. Technol.* 5 (1998) 16–28, <http://cecri.csircentral.net/id/eprint/2527>.
- [14] T. Arslan, F. Kandemirli, E.E. Ebenso, I. Love, A. Hailemichael, Quantum chemical studies on the corrosion inhibition of some sulphonamide on mild steel in acidic medium, *Corros. Sci.* 51 (2009) 35–47, <https://doi.org/10.1016/j.corsci.2008.10.016>.
- [15] N. Khalil, Quantum chemical approach of corrosion inhibition, *Electrochim. Acta* 48 (2003) 2635–2640, [https://doi.org/10.1016/S0013-4686\(03\)00307-4](https://doi.org/10.1016/S0013-4686(03)00307-4).
- [16] M. Rodriguez-ValdezL, A. Martinez-Villafane, D. Glossman-Mitnik, Computational simulation of the molecular structure and properties of heterocyclic organic compounds with possible corrosion inhibition properties, *J. Mol. Struct.* 713 (2005) 65–70, <https://doi.org/10.1016/j.theochem.2004.10.036>.
- [17] M.K. Awad, M.R. Mustafa, M.M.A. Elnga, Computational simulation of the molecular structure of some triazoles as inhibitors for the corrosion of metal surface, *J. Mol. Struct. (Theochem)*. 959 (2010) 66–74, <https://doi.org/10.1016/j.theochem.2010.08.008>.
- [18] I.B. Obot, N.O. Obi-Egbedi, E.E. Ebenso, A.S. Afolabi, E.E. Oguzie, Experimental, quantum chemical calculations, and molecular dynamic simulations insight into the corrosion inhibition properties of 2-(6-methylpyridin-2-yl)oxazolo [5,4-f] [1,10]phenanthroline on mild steel, *Res. Chem. Intermed.* 39 (2013) 1927–1948, <https://doi.org/10.1007/s11164-012-0726-3>.
- [19] A. Popova, M. Christov, Adsorption characteristics of corrosion inhibitors from corrosion rate measurements, *Corros. Sci.* 46 (2004) 1613–1620, [https://doi.org/10.1016/S0010-938X\(03\)00284-1](https://doi.org/10.1016/S0010-938X(03)00284-1).
- [20] A. Popova, M. Christov, S. Raicheva, E. Sokolova, Adsorption and inhibitive properties of benzimidazole derivatives in acid mild steel corrosion, *Corros. Sci.* 46 (2004) 1333–1350, <https://doi.org/10.1016/j.corsci.2003.09.025>.
- [21] H. Zhang, Y. Chen, Z. Zhang, Comparative studies of two benzaldehydethiosemicarbazone derivatives as corrosion inhibitors for mild steel in 1.0 M HCl, *Result Phys.* 11 (2018) 554–563, <https://doi.org/10.1016/j.rinp.2018.09.038>.
- [22] M. Talari, S.M. Nezhad, S.J. Alavi, M. Mohtashampour, A. Davoodi, S. Hosseinpour, Experimental and computational chemistry studies of two imidazole-based compounds as corrosion inhibitors for mild steel in HCl solution, *J. Mol. Liq.* 286 (2019) 110915, <https://doi.org/10.1016/j.molliq.2019.110915>.
- [23] J. Frau, D. Glossman-Mitnik, Conceptual DFT descriptors of amino acids with potential corrosion inhibition properties calculated with the latest Minnesota density functionals, *Front. Chem.* 5 (2017) 16, <https://doi.org/10.3389/fchem.2017.00016>.
- [24] N.O. Obi-Egbedi, N.D. Ojo, Computational studies of the corrosion inhibition potentials of some derivatives of 1H-imidazo [4,5-F][1,10] phenanthroline, *J. Sci. Res.* 14 (2015) 50–56, <https://scholar.google.co.za/citations?>
- [25] A.M. Ayuba, A. Uzairu, H. Abba, G.A. Shallangwa, Hydroxycarboxylic acids as corrosion inhibitors on aluminium metal: a computational study, *J. Mater. Environ. Sci.* 9 (2018) 3026–3034, <http://www.j.materenvirosci.com>.
- [26] N.P. Bellafont, F. Illas, P.S. Bagus, Validation of Koopmans' theorem for density functional theory binding energies, *Phys. Chem. Chem. Phys.* 17 (2015) 4015–4019, <https://doi.org/10.1039/C4CP05434B>.
- [27] A.A. Khadom, Quantum chemical calculations of some amines corrosion inhibitors/copper Alloy interaction in hydrochloric acid, *J. Mater. Environ. Sci.* 8 (2017) 1153–1160, <http://www.jmaterenvirosci.com>.
- [28] L.H. Madkour, I.H. Elshamy, Experimental and computational studies on the inhibition performances of benzimidazole and its derivatives for the corrosion of copper in nitric acid, *Int. J. Ind. Chem.* 7 (2016) 195–221, <https://doi.org/10.1007/s40090-015-0070-8>.
- [29] A.M. Ayuba, A. Uzairu, H. Abba, G.A. Shallangwa, Theoretical study of aspartic and glutamic acids as corrosion inhibitors on aluminium metal surface, *Moroc. J. Chem.* 6 (2018) 160–172, <http://revues.jmist.ma/?journal=morjchem&page=login>.
- [30] H. Lgaz, R. Salghi, A. Chaouiki, S. Shubhalaxmi, K.S. Jodeh, Bhat, Pyrazoline derivatives as possible corrosion inhibitors for mild steel in acidic media: a combined experimental and theoretical approach, *Cog. Eng.* 5 (2018) 1441585, <https://doi.org/10.1080/23311916.2018.1441585>.

- [31] L. Guo, Z.S. Safi, S. Kaya, W. Shi, B. Tüzün, N. Altunay, C. Kaya, Anticorrosive effects of some thiophene derivatives against the corrosion of iron: a computational study, *Front. Chem.* 6 (2018) 155, <https://doi.org/10.3389/fchem.2018.00155>.
- [32] P. Zhao, Q. Liang, Y. Li, Electrochemical, SEM/EDS and quantum chemical study of phthalocyanines as corrosion inhibitors for mild steel in 1 mol/L HCl, *Appl. Surf. Sci.* 252 (2005) 1596–1607, <https://doi.org/10.1016/j.apsusc.2005.02.121>.
- [33] M.K. Awad, Quantum chemical studies and molecular modelling of the effect of polyethylene glycol as corrosion inhibitors of an aluminium surface, *Can. J. Chem.* 91 (2013) 283–291, <https://doi.org/10.1139/cjc.2012-0354>.
- [34] M.E. Belghiti, Y. El Oudadi, S. Echihi, A. Elmelouky, H. Outada, Y. Karzazi, M. Bakasse, C. Jama, F. Bentiss, A. Dafali, Anticorrosive properties of two 3,5- disubstituted-4-amino-1,2,4-triazole derivatives on copper in hydrochloric acid environment: Ac impedance, thermodynamic and computational investigations, *Surf. Interf.* 21 (2020) 100692, <https://doi.org/10.1016/j.surfin.2020.100692>.
- [35] R.K. Roy, S. Pal, K. Hirao, On non-negativity of Fukui function indices, *J. Chem. Phys.* 110 (1999) 8236–8245, <https://doi.org/10.1063/1.478792>.
- [36] C. Morell, A. Grand, A. Toro-Labbe, Theoretical support for using the Delta f(r) descriptor, *Chem. Phys. Lett.* 425 (2006) 342–346, <https://doi.org/10.1016/j.cplett.2006.05.003>.
- [37] P. Geerlings, P.W. Ayers, A. Toro-Labbe, P.K. Chattaraj, F. De Proft, The Woodward–Hoffmann rules reinterpreted by conceptual density functional theory, *Acc. Chem. Res.* 45 (2012) 683–695, <https://doi.org/10.1021/ar200192t>.
- [38] G. Bereket, C. Ogretir, A. Yurt, Quantum mechanical calculations on some 4-methyl-5-substituted imidazole derivatives as acidic corrosion inhibitor for zinc, *J. Mol. Struct. (Theochem)*. 571 (2001) 139–145, [https://doi.org/10.1016/s0166-1280\(01\)00552-8](https://doi.org/10.1016/s0166-1280(01)00552-8).
- [39] U. Umaru, A.M. Ayuba, Quantum chemical calculations and molecular dynamic simulation studies on the corrosion inhibition of aluminium metal by myricetin derivatives, *J. New Technol. Mater.* 10 (2020) 18–28. <https://sites.google.com/site/jntmjournal/vol-10-issue2-dec-2020>.
- [40] O. Dagdag, A. El Harfi, M. El Gouri, Z. Safi, R.T. Jalgham, N. Wazzan, C. Verma, E.E. Ebenso, U.P. Kumar, Anticorrosive properties of Hexa (3-methoxy propan-1, 2-diol) cyclotriphosphazene compound for carbon steel in 3% NaCl medium: gravimetric, electrochemical, DFT and Monte Carlo simulation studies, *Heliyon* 5 (2019), e01340, <https://doi.org/10.1016/j.heliyon.2019.e01340>.
- [41] Y. Sasikumar, A.S. Adekunle, L.O. Olasunkanmi, I. Bahadur, R. Baskar, M.M. Kabanda, I.B. Obot, E.E. Ebenso, Experimental, quantum chemical and Monte Carlo simulation studies on the corrosion inhibition of some alkyl imidazolium ionic liquids containing tetrafluoroborate anion on mild steel in acidic medium, *J. Mol. Liq.* 211 (2015) 105–118, <https://doi.org/10.1016/j.molliq.2015.06.052>.
- [42] R.G. Pearson, Recent advances in the concept of hard and soft acids and bases, *J. Chem. Educ.* 64 (1987) 561, <https://doi.org/10.1021/ed064p561>.
- [43] M.E. Belghiti, S. Echihi, A. Mahsoune, Y. Karzazi, A. Aboulmouhajir, A. Dafali, I. Bahadur, Piperine derivatives as green corrosion inhibitors on iron surface; DFT, Monte Carlo dynamics study and complexation modes, *J. Mol. Liq.* 261 (2018) 62–75, <https://doi.org/10.1016/j.molliq.2018.03.127>.
- [44] S. Kaya, L. Guo, C. Kaya, B. Tüzün, I.B. Obot, R. Touir, et al., Quantum chemical and molecular dynamic simulation studies for the prediction of inhibition efficiencies of some piperidine derivatives on the corrosion of iron, *J. Taiwan Inst. Chem. Eng.* 65 (2016) 522–529, <https://doi.org/10.1016/j.jtice.2016.05.034>.
- [45] P. Banerjee, K.S. Sourav, G. Pritam, H. Abhiram, G.M. Naresh, Density functional theory and molecular dynamic simulation study on corrosion inhibition of mild steel by mercapto-quinoline Schiff base corrosion inhibitor, *Physica. E.* 66 (2015) 332–341, <https://doi.org/10.1016/j.physe.2014.10.035>.
- [46] G. Bereket, E. Hur, C. Ogretir, Quantum chemical studies on some imidazole derivatives as corrosion inhibitors for iron in acidic medium, *J. Mol. Struct. (Theochem)*. 578 (2002) 79–88, [https://doi.org/10.1016/S0166-1280\(01\)00684-4](https://doi.org/10.1016/S0166-1280(01)00684-4).
- [47] M.A. Quraishi, R. Sardar, Hector bases – a new class of heterocyclic corrosion inhibitors for mild steel in acid solutions, *J. Appl. Electrochim.* 33 (2003) 1163–1168, <https://doi.org/10.1023/B:JACH.0000003865.08986.fb>.
- [48] U. Umaru, A.M. Ayuba, Computational study of anticorrosive effects of some thiazole derivatives against the corrosion of aluminium, *RHAZES: Green Appl. Chem.* 10 (2020) 113–128, <https://doi.org/10.48419/IMIST.PRSM/rhazes-v10.23814>.
- [49] S. Martinez, Inhibitory mechanism of mimosa tannin using molecular modeling and substitutional adsorption isotherms, *Mater. Chem. Phys.* 77 (2003) 97–102, [https://doi.org/10.1016/S0254-0584\(01\)00569-7](https://doi.org/10.1016/S0254-0584(01)00569-7).
- [50] C.B. Verma, M.A. Quraishi, A. Singh, 2-Aminobenzene-1,3-dicarbonitriles as green corrosion inhibitor for mild steel in 1 M HCl: electrochemical, thermodynamic, surface and quantum chemical investigation, *J. Taiwan. Inst. Chem. Eng.* 49 (2015) 229–239, <https://doi.org/10.1016/j.jtice.2014.11.029>.
- [51] I. Lukovits, E. Kalman, F. Zucchi, Corrosion inhibitors - correlation between electronic structure and efficiency, *Corros* 57 (2001) 3–8, <https://doi.org/10.5006/1.3290328>.
- [52] B. Gómez, N.V. Likhanova, M.A. Domínguez-Aguilar, R. Martínez-Palou, A. Vela, J.L. Gazquez, Quantum chemical study of the inhibitive properties of 2-pyridyl-azoles, *J. Phys. Chem. B* 110 (2006) 8928–8934, <https://doi.org/10.1021/jp057143y>.
- [53] M.A. Bedair, The effect of structure parameters on the corrosion inhibition effect of some heterocyclic nitrogen organic compounds, *J. Mol. Liq.* 219 (2016) 128–141, <https://doi.org/10.1016/j.molliq.2016.03.01>.